Spatial Consistency of Multipath Components in a Typical Urban Scenario

Fjolla Ademaj and Stefan Schwarz

Christian Doppler Laboratory for Dependable Wireless Connectivity for the Society in Motion
TU Wien, Institute of Telecommunications, Gusshausstrasse 25/389, A-1040 Vienna, Austria
Email: {fjolla.ademaj, stefan.schwarz}@tuwien.ac.at,

***Abstract*—Channel models should be accurate in reflecting a realistic behavior between transmitter and receiver. To be able to capture smooth variations of channels, i.e., when a user moves, or when multiple users are close to each other in a confined area, channels should include spatial correlation. There are various applications that make use of these smooth channel variations including beam tracking strategies and beam forming strategies based on angular information. In this paper we show a spatially consistent geometry-based channel model and compare it to a deterministic ray-tracing model. Characteristics of strongest multipath components in terms of delay and angles of arrival in azimuth and elevation over consecutive spatial locations in an urban environment, are evaluated. Our model for spatial consistency reveals a realistic behaviour and statistically is capable to mimic the appearance of new scatterers and disappearance of old ones, thus matching the outcome of ray-tracing modeling.**

***Index Terms*—channel model, spatial correlation, ray-tracing, beam forming, decorrelation distance, urban scenario, multipath components.**

I. Introduction

Channel models are an important component that affects the evaluated performance of various techniques and technologies in wireless communications. Therefore, in order to come to a sensible and accurate evaluation, channel models should reflect a realistic behaviour of the environment between transmitter and receiver. In the last years, the focus on new techniques such as full dimension (FD)-multiple input multiple output (MIMO), 3-dimensional (3D) beamforming has opened new questions and demands in terms of channel models to be used [1], [2]. Thus, from simple power delay profile (PDP)-based channel models that impose very low complexity when used in simulation tools, the attention shifted towards more complex channels models that incorporate not only a PDP, but also a statistical angular profile (AP) to characterize multipath components. Examples of such channel models are the 3rd Generation Partnership Project (3GPP) 3D channel model specified in study items TR 36873 [3] and TR 38901 [4] feasible for frequencies ranging from 0.5 to $100\,\mathrm{GHz}$.

A fundamental aspect of wireless cellular networks is that they allow for mobility of the users. In this regard, the propagation environment changes gradually therefore it is expected that the channel models reflect the spatial correlation. This is important especially in massive MIMO scenarios, beam tracking and beam forming strategies that are based on user location and angular information, i.e., multi-layer precoding [5]–[7].

Most of the existing spatial channel models are relevant only for drop-based simulations, where all channel parameters are fixed for a given user location that is static. Any movement is only performed virtually where only the Doppler effect evolves. Such drop-based models are popular in Monte Carlo simulations, however they produce non-realistic and inaccurate results in absence of spatial consistency. Spatial consistency has become a critical modeling component in the standardization bodies e.g., 3GPP, and alternatives to extend the 3GPP 3D and millimeter wave (mmWave) channel models are provided in the recent 3GPP TR38901. In our previous work in [8] we have introduced a generic model for spatial consistency, applicable to all geometry-based stochastic channel models. Given that the model is analytic and its key parameter is *decorrelation distance*, a parameter that relates to the physical distance between spatial points, it is necessary to determine the range of values for this parameter that deliver a realistic performance. Following a statistical approach and hypothesis testing our model for spatial consistency is validated in [9] and decorrelation distance values are derived.

In this paper we use a ray-tracing tool to perform simulations in an urban environment and evaluate the behaviour of strongest multipath components over consecutive spatial positions. Similarly, by using our model for spatial consistency from [8], [9] we observe parameters like multipath delay and angle of arrival in azimuth and elevation. The main intention is to see if our model is capable of capturing a death-birth process of scatterers along the propagation path.

II. Channel Models

Based on the applied modeling approach, channel models can be broadly classified in three categories: *deterministic*, *stochastic* and *geometry-based stochastic* channel models.

- Deterministic models describe the propagation channel for a specific environment with specific location of transmitters and receivers. Examples of such models are ray tracing simulations based on 3D-building models. These models can provide very accurate performance predictions for their specific scenarios as long as all scenario

information is available in high precision. However, being related only to very specific scenarios, these models do not allow for general statements.

- Stochastic channel models are independent of a particular environment and can be used to generate an essentially unlimited amount of channel realizations with the desired statistical properties. The physical parameters (power delay profile, angular profile) are determined in a completely stochastic way by prescribing probability distribution functions without assuming an underlying geometry.
- Geometry-based models can be seen as a balance between the two extremes of purely deterministic and purely stochastic channel modeling. The location of scatterers is not explicitly specified, instead the multipath directions generated as a result of scattering objects are considered. Specific multipath properties (e.g., direction, power, delay) are parametrized by means of distributions and thus determined stochastically. On the other side, the propagation parameters are determined according to the geometric positions of the transmitter and receiver. Such models are frequently adopted by standardization bodies such as the 3GPP, IEEE or ITU.

A. Ray-Tracing Simulator

In this paper we use a 3D ray-tracing simulator [10], developed by Beijing Jiaotong University, to conduct simulations of a deterministic typical urban environment. The ray-tracing simulator is composed of a geometrical representation of the simulated scenario/environment which is the input to the simulator. We use a 3D modeling computer program named Sketchup to construct the 3D environment. Based on the geometry of the environment, that is used as input to the ray-tracing, as well as location of transmitter and receiver, all ray paths are determined. The ray paths with their corresponding electromagnetic properties are considered for calculating and determining the complex field strengths of the multipath components. These calculations comprise of the free space loss, reflection losses as well as various diffuse scattering models such as the Kirchhoff and Lambertian scattering models [11], [12]. Since the locations of the scatterers in a simulated environment are known, consequently the channel characteristics from a ray-tracing simulator are spatially consistent.

B. 3GPP 3D Channel Model

The 3GPP 3D channel model specified in TR 36.873 is a 3D geometry-based stochastic model, describing the scattering environment between transmitter and receiver in both azimuth and elevation dimensions. The model uses statistically generated environments with scattering clusters that individually reflect multipath components. It includes *large-scale parameters* (shadow fading, Ricean K-factor, delay spread, azimuth angle spread of departure- and arrival, as well as zenith angle spread of departure- and arrival) and *small-scale parameters* (delays, cluster powers as well as angles of departure and -arrival in azimuth and elevation direction) [3], [13]. The large-scale

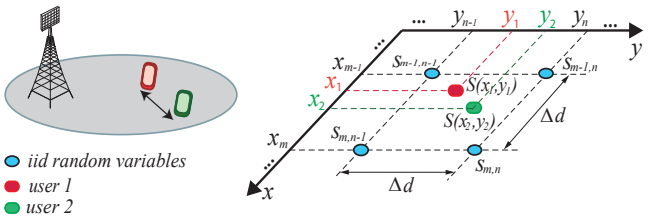

Fig. 1. Spatially correlated random variables based on a 2-dimensional (2D) grid of independent and identically distributed (iid) random variables denoted by blue dots. The grid has a specific resolution denoted by Δd.

parameters incorporate the geometric position of the transmitter and receiver, and are used to parametrize the distribution functions that generate the small-scale parameters. For each spatial position in the 3D environment, independent random variables are generated. Since the scattering environment is defined by means of these independent random variables, this leads to a completely different scattering environment for every spatial position, thus making the model spatially inconsistent.

III. Spatial Consistency

In our previous work in [8, Sec.IV], we have extended the 3GPP compliant step-wise small-scale parameter generation (see [13] for a more detailed description) by introducing a new step to generate spatially correlated random variables. The intention is not to modify or destroy the statistical properties of the channel model itself, but rather to only establish the generation of random variables in a way such that the resulting small-scale parameters provide spatial correlation. Our model to generate spatially correlated small-scale parameters works as follows:

1) Generate a matrix $\mathbf{S}$ of iid random variables according to tabulated distributions (e.g., $\mathcal{U}(0,1)$ for delay, $\mathcal{N}(0,\sigma^2_{\mathrm{AS}})$ for angular variation, see [8, Table I]);
2) Define a mapping between user positions (x,y) and entries of matrix $\mathbf{S}$, (e.g., $S_{m-1,n-1}, S_{m-1,n}, S_{m,n-1}, S_{m,n}$, see Fig. 1);
3) Apply bilinear interpolation to get the interpolated random variable from matrix $\mathbf{S}$ for the corresponding user position $\tilde{S}(x,y)$;

The size of matrix $\mathbf{S}$ corresponds to the entire simulation area where the users are located and it has a certain resolution denoted by the parameter, Δd. The parameter Δd represents the decorrelation distance, which relates to the physical distance between users and represents the resolution of the iid random variables. Thus, by choosing different values of Δd, the model yields different correlation levels of channel parameters.

Based on a statistical approach utilizing ray-tracing simulations and by performing hypothesis testing, the decorrelation distance is parametrized in [9]. For a typical urban environment, complementary to the 3GPP 3D-urban macro cell (UMa) scenario from [3], the parametric values of decorrelation distance are summarized in Table I. It is observed that the value of decorrelation distance depends strongly on the propagation

TABLE I. The parametric values of decorrelation distance [9].

	LOS	NLOS
AoA	$\Delta d = 10$	$\Delta d = 20$
EoA	$\Delta d = 5$	$\Delta d = 10$

condition, i.e., line-of-sight (LOS) or non line-of-sight (NLOS) and it also differs between channel parameters, i.e., azimuth of arrival (AoA) results with a higher value of Δd compared to elevation of arrival (EoA).

A. Small-scale parameter correlation

In the step-wise generation procedure of small-scale parameters within the 3GPP 3D channel model, delays are drawn randomly form the delay distribution defined in [3, Tab. 7.3-6]. Considering an exponential delay distribution, the delay for each cluster is defined as

$$\tau_k = -r_\tau \sigma_{\mathrm{DS}} \ln(\mathrm{X_k}), \tag{1}$$

where r_τ is the delay proportionality factor, σ_{DS} denotes the delay spread, $k = 1, ...K$ is the cluster index and $X_k \sim \mathcal{U}(0,1)$ is the random variable that needs to be correlated.

By applying our model model for spatial consistency as described above, instead of variable X_k, a matrix $\mathbf{S}_k$ with entries $S_{k_{m,n}} \sim \mathcal{U}(0,1)$ is generated and then based on the bilinear interpolation between entries of matrix $\mathbf{S}_k$ for the corresponding user position x, y, the correlated random variable $\tilde{S}_k(x,y)$ is used. Thus, equation (1) now becomes,

$$\tau_k = -r_\tau \sigma_{\mathrm{DS}} \ln\left(\tilde{\mathrm{S}}_\mathrm{k}(\mathrm{x},\mathrm{y})\right). \tag{2}$$

Similarly, for generation of arrival and departure angles for both azimuth and elevation (Step 7 in TR 36873), the following equations apply,

$$\phi_{k,\mathrm{AOA}} = \tilde{P}_k(x,y)\phi'_{k,\mathrm{AOA}} + \tilde{Q}_k(x,y) + \phi_{\mathrm{LOS,AOA}}, \tag{3}$$

$$\theta_{k,\mathrm{EOA}} = \tilde{X}_k(x,y)\theta'_{k,\mathrm{EOA}} + \tilde{Y}_k(x,y) + \theta_{\mathrm{LOS,EOA}}. \tag{4}$$

The parameters $\phi'_{k,\mathrm{AOA}}$ and $\theta'_{k,\mathrm{EOA}}$ are defined with respective functions from tabulated distributions in [3] for azimuth and elevation and do not include any randomness. The variables $\tilde{P}_k(x,y)$, $\tilde{Q}_k(x,y)$, $\tilde{X}_k(x,y)$ and $\tilde{Y}_k(x,y)$ denote correlated random variables for the corresponding distributions. For example, in equation (3), $\tilde{P}_k(x,y)$ represents the interpolated value from entries $P_{k_{m,n}} \sim \mathcal{U}(\{-1,1\})$ of matrix $\mathbf{P}$. This follows the specifics of the 3GPP TR 36873, where instead, a random variable with uniform distribution on a discrete set is defined. It is important to note that during the generation of small-scale parameters, it is not sufficient to generate only one matrix/grid or random variables, but rather as many matrices as there are distributions defined, e.g., as in our illustration with matrices **S**, **P**, **Q**, **X** and **Y** that follow different distributions.

IV. Simulation Results

Using the 3GPP 3D channel model [13] extended with the spatial consistency feature described in Section III we perform simulations and analyse the behaviour of the strongest

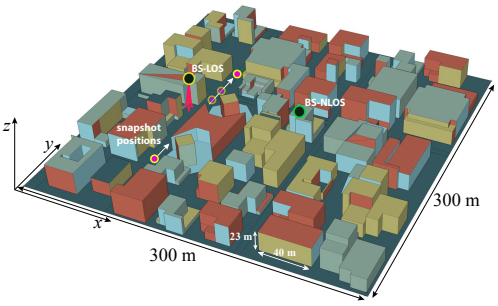

(a)

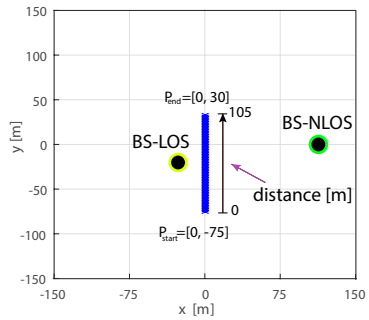

(b)

Fig. 2. Urban scenario: (a) the constructed scenario in 3D used in ray-tracing tool denoting base station positions and receive snapshot positions in LOS and NLOS, (b) the corresponding geometry in 2D used with the 3GPP 3D channel model. The size of the scenario and corresponding transmitter- and receiver positions are the same for both cases.

TABLE II. Simulation parameters

Parameter	Value
Transmitter height	25m
Receiver height	1.5 m
Avg. building height	20 m
Avg. street width	20 m
Antenna pattern	omni-directional
Carrier frequency	3.5 GHz

multipath components over consecutive spatial locations. The focus in this paper is on urban enviornemts, thus we select the UMa scenario from [3]. For comparison, we construct a scenario geometry that represents a typical urban environment, as illustrated in Fig. 2, and perform simulations with the ray-tracing tool from [10]. In order to keep the comparison fair, in both channel models, 3GPP 3D model and ray-tracing, the parameters from Table II are applied. Individually, LOS and NLOS propagation conditions are analysed, thus two different transmitter locations are chosen. The location of transmit and receive snapshot positions are illustrated in Fig. 2. Only one transmitter is considered during one simulation with a fixed propagation condition (for the 3GPP 3D model), assuming no interference. Different material types for the constructed scenario are chosen from the material database provided in ray-tracing. Various colors in Fig. 2 represent different materials used, e.g., brick, redbrick, glass, wood, tiles etc.

The length of snapshots recorded on the receive locations along the propagation path is 105 m, with a resolution every one meter. We focus on three different characteristics of

multipath components: normalized delay, AoA and EoA. The definition of normalized delay is the miltpath delay subtracted with the delay of the direct path. Since in ray-tracing the number of multipath components is very high, we consider only the strongest ones. The behaviour of the direct path and the strongest multipath when considering LOS is shown in Fig. 3. Ray-tracing results in Fig. 3 (a), (b) and (c) reveal a smooth behaviour of delay, AoA and EoA over spatial locations for the direct path[1], following the geometry of transmit-receive locations. When looking at the first strongest multipath component, as expected, the behaviour is more disruptive over spatial locations due to scattering effects. Especially, more intersperse changes are noticed at the locations where receive points are close to transmitter and there are more changes in the surfaces of buildings around, causing new scatterers to appear. On the other side, the results from the 3GPP 3D model, Fig. 3 (d)- (f), indicate a similar behaviour when using spatial consistency with parametrized values for decorrelation distance from [9]. The model uses a statistical approach, so the scattering objects will not follow the exact behaviour as in ray-tracing, however the model reveals similar characteristics as if new scatterers would arise and old ones would disappear. In contrary to our extended model, the results of the 3GPP 3D model without spatial consistency (green line in Fig. 3 (d), (e) and (f)) show very large fluctuations along consecutive spatial positions resulting in a spatially inconsistent model.

Similarly, the results for NLOS propagation condition are shown in Fig. 3 (g)- (l). Compared to the behaviour in LOS, we notice more changes in terms of normalized delay, AoA and EoA over consecutive spatial positions that are true for ray-tracing as well as the 3GPP 3D model with spatial consistency. One thing to note is that for the multipath delay we consider two values of decorrelation distance, since a parametrization of the model for the delay parameter is not done yet. The impact of the decorrelation distance value is clearly visible, where with a smaller Δd, more changes appear over spatial locations resembling on a propagation environment that changes more quickly.

V. Conclusion

We have shown a spatially consistent geometry-based channel model by considering the 3GPP 3D model as an example and compared with a ray-tracing deterministic model. Analysing characteristics of strongest multipath components over consecutive spatial positions, good agreement between the two models is observed. Individually, LOS and NLOS propagation conditions are evaluated. Using already parametrized values of decorrelation distance, our model reveals similar characteristics with ray-tracing, in terms of spatial correlation, as if new scatterers would arise and old ones would disappear.

[1]Note that in the last spatial positions the direct path shows some chnages, because the receive locations are not in LOS anymore and the penetration loss is considered.

Acknowledgment

This work has been funded by the Christian Laboratory for Dependable Wireless Connectivity for the Society in Motion. The financial support by the Austrian Federal Ministry for Digital and Economic Affairs and the National Foundation for Research, Technology and Development is gratefully acknowledged.

References

[1] T. L. Marzeta, *Fundamentals of Masive MIMO*, 1st ed. Cambridge University Press, Nov. 2016, ISBN: 978-1-107-17557-0.

[2] E. Bjornson, J. Hoydis, and L. Sanguinetti, "Massive MIMO Networks: Spectral, Energy, and Hardware Efficiency," *Foundations and Trends in Signal Processing*, vol. 11, no. 3-4, pp. 154–655, 2017, ISSN: 1932-8346. DOI: 10.1561/2000000093. [Online]. Available: http://dx.doi.org/10.1561/2000000093.

[3] 3. G. P. P. (3GPP), "Study on 3D channel model for LTE," 3rd Generation Partnership Project (3GPP), TR 36.873, Sep. 2014.

[4] ——, "Study on channel model for frequencies from 0.5 to 100GHz," 3rd Generation Partnership Project (3GPP), TR 38.901, Dec. 2017.

[5] S. Schwarz, "Robust full-dimension MIMO transmission based on limited feedback angular-domain CSIT," *EURASIP Journal on Wireless Communications and Networking*, vol. 2018, no. 1, pp. 1–20, Mar. 2018.

[6] A. Alkhateeb, G. Leus, and R. W. Heath, "Multi-layer precoding for full-dimensional massive MIMO systems," in *48th Asilomar Conference on Signals, Systems and Computers*, Nov. 2014, pp. 815–819. DOI: 10.1109/ACSSC.2014.7094563.

[7] S. Schwarz and M. Rupp, "Society in motion: challenges for LTE and beyond mobile communications," *IEEE Communications Magazine*, vol. 54, no. 5, pp. 76–83, May 2016, ISSN: 0163-6804. DOI: 10.1109/MCOM.2016.7470939.

[8] F. Ademaj, M. K. Müller, S. Schwarz, and M. Rupp, "Modeling of Spatially Correlated Geometry-Based Stochastic Channels," in *2017 IEEE 86th Vehicular Technology Conference (VTC-Fall)*, Sep. 2017, pp. 1–6. DOI: 10.1109/VTCFall.2017.8287884.

[9] F. Ademaj, S. Schwarz, K. Guan, and M. Rupp, "Ray-Tracing based Validation of Spatial Consistency for Geometry-Based Stochastic Channels," in *2018 IEEE 88th Vehicular Technology Conference (VTC-Fall)*, in press, Aug. 2018, pp. 1–5.

[10] , http://raytracer.cloud/.

[11] D. He, B. Ai, K. Guan, L. Wang, Z. Zhong, and T. Kürner, "The design and applications of high-performance ray-tracing simulation platform for 5g and beyond wireless communications: A tutorial," *IEEE Communications Surveys Tutorials*, pp. 1–1, 2018, ISSN: 1553-877X. DOI: 10.1109/COMST.2018.2865724.

[12] K. Guan, X. Lin, D. He, B. Ai, Z. Zhong, Z. Zhao, D. Miao, H. Guan, and T. Kürner, "Scenario modules and ray-tracing simulations of millimeter wave and terahertz channels for smart rail mobility," in *2017 11th European Conference on Antennas and Propagation (EUCAP)*, Mar. 2017, pp. 113–117. DOI: 10.23919/EuCAP.2017.7928471.

[13] F. Ademaj, M. Taranetz, and M. Rupp, "3GPP 3D MIMO Channel Model: A holistic implementation guideline for open source simulation tools," *EURASIP Journal on Wireless Communications and Networking*, 2016. DOI: 10.1155/2007/19070.

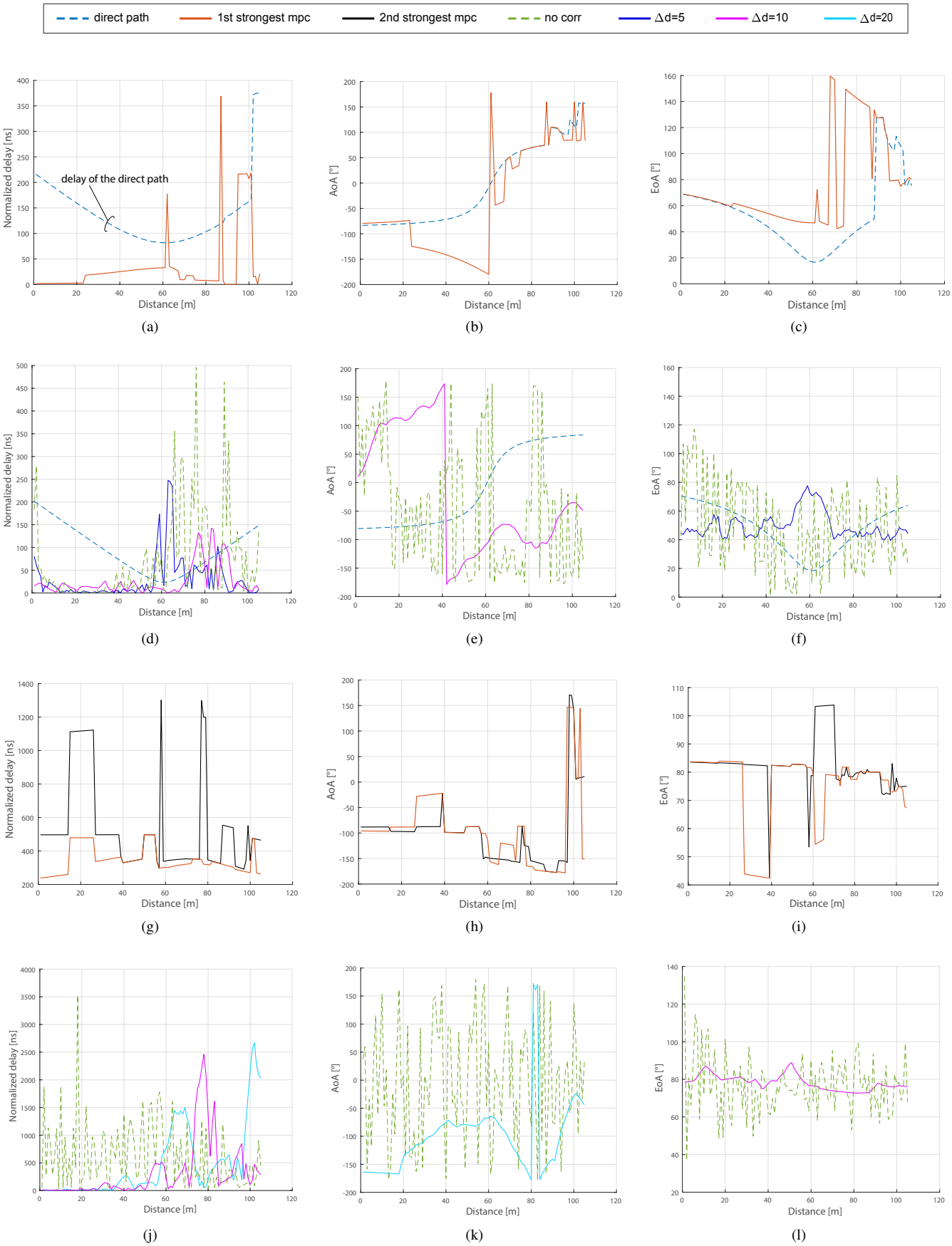

Fig. 3. Characteristics of the direct path and the strongest multipath components for spatial positions in LOS and NLOS propagation condition. The ray-tracing results considering the direct path and the first strongest multipath component for LOS are shown in (a) normalized delay, (b) AoA and (c) EoA and for NLOS are shown in (g) normlaized delay, (h) AoA and (i) EoA. The results from 3GPP 3D model for LOS case are shown in (d) normalized delay, (e) AoA and (f) EoA and for NLOS case in (j) normalized delay, (k) AoA and (l) EoA, assuming the case without spatial consistency and with spatial consistency for parametrized values of decorrelation distance (Δd).